

# Spectral Function in Mott Insulating Surfaces

L. O. Manuel<sup>1</sup>, C. J. Gazza<sup>1</sup>, A. E. Feiguin<sup>2</sup>, and A. E. Trumper<sup>1</sup>

<sup>1</sup>*Instituto de Física Rosario (CONICET) and Universidad Nacional de Rosario,  
Boulevard 27 de Febrero 210 bis, (2000) Rosario, Argentina*

<sup>2</sup>*Department of Physics and Astronomy, University of California, Irvine, California 92697*

(Dated: February 7, 2020)

We show theoretically the fingerprints of a magnetic  $120^\circ$  Néel order in the photoemission spectra of the Mott insulating ground states realized in the  $\sqrt{3} \times \sqrt{3}$  triangular silicon surfaces K/Si(111)-B and SiC(0001). The calculated spectra present low energy features of magnetic origin with a reduced dispersion  $\sim 10 - 40$  meV compared with the center-of-mass spectra bandwidth  $\sim 0.2 - 0.3$  eV. Remarkably, we find that the quasiparticle signal survives only around the magnetic Goldstone modes. We propose angle-resolved photoemission experiments as an indirect determination of the existence of long range magnetic order in these surfaces. Our findings would position these silicon surfaces as new candidates to investigate non-conventional quasiparticle excitations.

It is well known that the strong correlation in electronic systems with an odd number of electrons per unit cell may give rise to Mott insulating (MI) ground states, in contradiction with band theory predictions. Generally, the presence of metal-transition ions with unpaired electrons are responsible for the MI properties of many compounds like the undoped high- $T_c$  cuprates. However, it has also been shown that surfaces characterized by a  $\sqrt{3} \times \sqrt{3}$  arrangement of silicon dangling-bond surface orbitals can provide the ideal conditions to realize the MI phenomena without metal-transition ions[1, 2, 3, 4]. Although the on-site Coulomb potential  $U$  is not so large, the surface state bandwidth is reduced due to reconstructions, becoming the correlation effect important. Recently, Weitering *et al.*[1] used moment-resolved direct and inverse photoemission spectroscopy to demonstrate that the triangular interface K/Si(111)-( $\sqrt{3} \times \sqrt{3}$ )-B (hereafter K/Si-B) has a MI ground state. Even though such an insulating state is not necessarily unstable toward antiferromagnetism due to the lack of perfect nesting, it has also been argued that K/Si-B is the first experimental realization of a triangular Heisenberg spin-1/2 model with a  $120^\circ$  Néel order. However, standard density-functional methods combined with exact diagonalization studies suggest a Mott insulator with a non-magnetic ground state[5]. In addition, it was speculated that the reconstructed triangular surface SiC(0001)-( $\sqrt{3} \times \sqrt{3}$ ) [2] (hereafter SiC) also presents a  $120^\circ$  Néel ordered ground state[3]. Since direct measurements of long range order in such surfaces are difficult to implement, the magnetic properties of these MI ground states still remain unanswered[3]. On the other hand, nowadays it is possible to perform higher resolution photoemission experiments than the previous ones, which would allow a detailed analysis of the single-hole properties in these MI ground states. These issues motivated us to study theoretically the single-hole dynamics in a triangular antiferromagnet (AF) with two objectives: i) to investigate the effect of a frustrated magnetic order in the quasiparticle (QP) behavior, and ii) to obtain spectro-

scopic fingerprints of long-range magnetic order through the photoemission spectra calculated for realistic parameters of the surfaces K/Si-B and SiC. A careful comparison with future higher resolution spectroscopy experiments could give an indirect evidence for the existence, or not, of the  $120^\circ$  magnetic ordered ground state.

As a consequence of the magnetic order, we find a strong  $k$ -dependence of the spectral function structures. In particular, we show the emergence of spectral weight of magnetic origin between the Fermi level and the measured surface state band, with a strongly reduced dispersion. For the surfaces K/Si-B and SiC, our results show a remarkable vanishing of the QP weight for a large region of the Brillouin zone (BZ) outside a neighborhood of the magnetic Goldstone modes. For decades researchers have tried to look for spin-liquid phases that upon hole doping, give rise to non-conventional excitations[6]. Now we give firm evidence that such non-conventional excitations can be found in *non-collinear* spin-crystal phases like the one we propose for the MI silicon surfaces.

To tackle this problem we assume the  $t - J$  model, which is supposed to capture the low-energy physics involved in photoemission spectroscopy of antiferromagnetic Mott insulators[7]. In order to solve the model, we use the self-consistent Born approximation (SCBA) complemented with exact diagonalization studies. For non-frustrated AF, it has already been established the success of the SCBA to reproduce exact diagonalization results on small clusters[8] and angle-resolved photoemission spectroscopy (ARPES) experiments[7].

As our interest is to find indirect evidence of long-range magnetic order in the spectroscopic data, we assume a surface ground state with a magnetic wave vector  $\mathbf{Q} = (4\pi/3, 0)$  lying in the surface plane  $x - z$ , and spin waves as the low energy excitations. We perform a unitary transformation to local quantization axis so as to have a ferromagnetic ground state in the  $z'$  direction. Then, we use the spinless fermion  $\hat{c}'_{i\uparrow} = h_i^\dagger$ ,  $\hat{c}'_{i\downarrow} = h_i S_i^-$ , and the Holstein-Primakov  $S_i^{x'} \sim \frac{1}{2}(a_i^\dagger + a_i)$ ,

$S_i^{y'} \sim \frac{i}{2}(a_i^\dagger - a_i)$ ,  $S_i^{z'} = \frac{1}{2} - a_i^\dagger a_i$  representations. These are replaced in the  $t$ - $J$  model keeping the relevant terms up to third order. After a lengthy but straightforward calculation, the Hamiltonian results

$$H = \sum_{\mathbf{k}} \epsilon_{\mathbf{k}} h_{\mathbf{k}}^\dagger h_{\mathbf{k}} + \sum_{\mathbf{q}} \omega_{\mathbf{q}} \alpha_{\mathbf{q}}^\dagger \alpha_{\mathbf{q}} - t \sqrt{\frac{3}{N_s}} \sum_{\mathbf{k}, \mathbf{q}} \left[ M_{\mathbf{kq}} h_{\mathbf{k}}^\dagger h_{\mathbf{k}-\mathbf{q}} \alpha_{\mathbf{q}} + h.c. \right]. \quad (1)$$

In the Hamiltonian (1),  $\epsilon_{\mathbf{k}} = -t\gamma_{\mathbf{k}}$  and  $\omega_{\mathbf{q}} = \frac{3}{2}J\sqrt{(1-3\gamma_{\mathbf{q}})(1+6\gamma_{\mathbf{q}})}$  are the hole and magnon dispersions, respectively.  $\gamma_{\mathbf{k}} = \sum_{\delta} \cos(\mathbf{k} \cdot \delta)$  and  $\beta_{\mathbf{k}} = \sum_{\delta} \sin(\mathbf{k} \cdot \delta)$  are geometric factors, with  $\delta$  the positive vectors to nearest neighbors, and  $\mathbf{k}$  varying in the first BZ of the  $\sqrt{3} \times \sqrt{3}$  surface. The bare hole-magnon vertex interaction is defined by  $M_{\mathbf{kq}} = i(\beta_{\mathbf{k}} v_{-\mathbf{q}} - \beta_{\mathbf{k}-\mathbf{q}} u_{\mathbf{q}})$  with the Bogoliubov coefficients  $u_{\mathbf{q}} = [(1+3\gamma_{\mathbf{q}}/2 + \omega_{\mathbf{q}})/2\omega_{\mathbf{q}}]^{\frac{1}{2}}$  and  $v_{\mathbf{q}} = \text{sign}(\gamma_{\mathbf{q}}) [(1+\gamma_{\mathbf{q}}/2 - 3\omega_{\mathbf{q}})/2\omega_{\mathbf{q}}]^{\frac{1}{2}}$ . The free hopping hole term implies a finite probability of the hole to move without emission or absorption of magnons because of the underlying *non-collinear* magnetic structure. The hole-magnon vertex interaction adds another mechanism for the charge carrier motion which is magnon-assisted. The latter is the responsible for the spin-polaron formation when a hole is injected in a non-frustrated antiferromagnet[8, 9]. A priori, the formation of the spin-polaron would be enhanced by the free hopping term. We will show, however, the existence of a subtle interference between both processes that turns out to be dependent on the surface band structure. An important quantity that allows us to study the interplay between such processes is the retarded hole Green function that is defined as  $G_{\mathbf{k}}^h(\omega) = \langle AF | h_{\mathbf{k}} \frac{1}{\omega + i\eta^+ - H} h_{\mathbf{k}}^\dagger | AF \rangle$ , where  $|AF\rangle$  is the undoped antiferromagnetic ground state with a  $120^\circ$  Néel order. In the SCBA the self energy at zero temperature results

$$\Sigma_{\mathbf{k}}(\omega) = \frac{3t^2}{N_s} \sum_{\mathbf{q}} \frac{|M_{\mathbf{kq}}|^2}{\omega - \omega_{\mathbf{q}} - \epsilon_{\mathbf{k}-\mathbf{q}} - \Sigma_{\mathbf{k}-\mathbf{q}}(\omega - \omega_{\mathbf{q}})}.$$

We have solved numerically this self-consistent equation for  $\Sigma_{\mathbf{k}}(\omega)$ , and calculated the hole spectra function  $A_{\mathbf{k}}(\omega) = -\frac{1}{\pi} \text{Im} G_{\mathbf{k}}^h(\omega)$  and the quasiparticle (QP) weight  $z_{\mathbf{k}} = \left(1 - \frac{\partial \Sigma_{\mathbf{k}}(\omega)}{\partial \omega}\right)^{-1} |_{E_{\mathbf{k}}}$ , where the QP energy is given by  $E_{\mathbf{k}} = \Sigma_{\mathbf{k}}(E_{\mathbf{k}})$ . Before we discuss the results it is important to mention that, unlike previous works[10], we will concentrate on the behavior of the photoemission spectra for realistic parameters of the surfaces K/Si-B and SiC, what implies a strong coupling regime and a careful extrapolation to the thermodynamic limit[11].

For the K/Si-B (SiC) surface, photoemission spectra give a bandwidth  $W \sim 0.3$  eV ( $\sim 0.2$  eV) for the occupied surface electronic band[1, 2]. These experiments

together with inverse photoemission indicate an effective on-site Coulomb repulsion  $U \sim 1-2$  eV ( $\sim 1.5-2$  eV). Electronic band calculations give a similar value for  $U$  and a wider surface bandwidth  $W \sim 0.61$  eV ( $\sim 0.35$  eV), due to the neglection of correlation effects, leading to a *positive*  $t \sim 0.07$  eV ( $\sim 0.04$  eV) [4, 5]. The large  $U/W$  ratios indicate the presence of strong electronic correlations and a considerable suppression of charge fluctuations. In addition, scanning tunneling microscopy measurements on the SiC surface show a clear evidence of a Mott insulating state[12]. Theoretical works on the Hubbard model suggest that these surfaces would be located in the antiferromagnetic region of the phase diagram[13]. All these estimations point out to  $J/t \sim 0.1-0.4$  for both surfaces. In that parameter range, we have observed negligible quantitative changes in our results, so we take  $J/t = 0.4$  as a reference value.

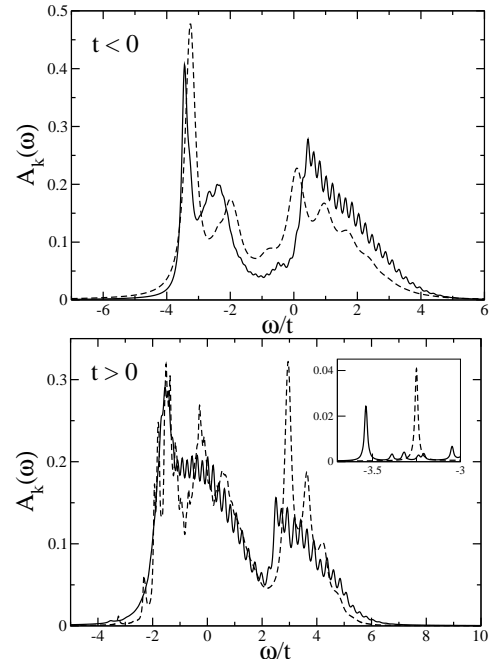


FIG. 1: Spectral functions versus frequency for  $J/|t| = 0.4$  and  $N = 21$  corresponding to a  $\mathbf{k}$  in the interior of the BZ. The solid and dashed lines are the exact and SCBA results, respectively. The inset shows the low energy sector.

In order to test the validity of the SCBA we have compared its results for the single-hole dynamics with Lanczos exact diagonalization (ED) calculations on small clusters. In general, we have found a good agreement for all momenta of the BZ and for  $J/t \lesssim 1$ . In Fig. 1 we show the spectral function for a cluster size of  $N = 21$  and in the strong coupling regime  $J/|t| = 0.4$ , for both signs of  $t$  and a generic  $\mathbf{k}$  of the BZ. There is an excellent agreement between ED and SCBA results in the whole range of energies. Regarding the low-energy features, we have observed that a change of the  $t$  sign, from negative to positive, induces a sizable decrease in the QP weight  $z_{\mathbf{k}}$

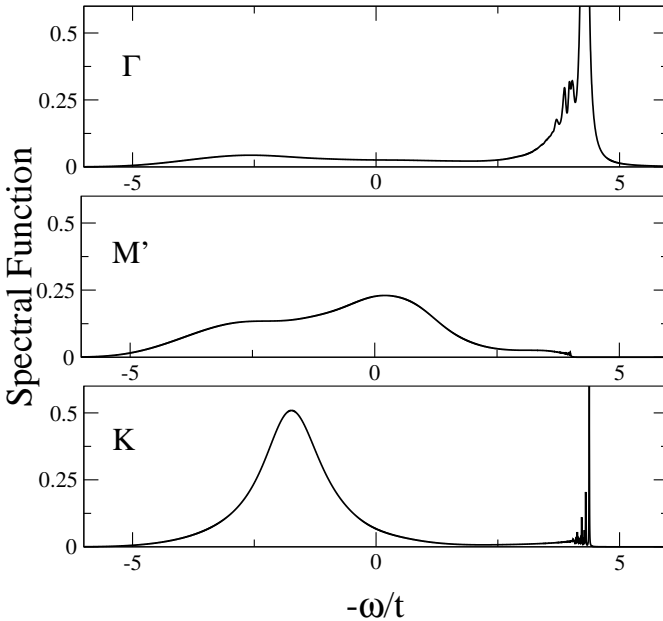


FIG. 2: Spectral functions for realistic parameters of the silicon surfaces ( $J/t = 0.4$ ) calculated at three different points of the BZ (see inset Fig. 3). Notice that the Fermi level has been placed on the right.

(compare the low-energy peak in the upper panel and the inset of Fig. 1) for almost all  $\mathbf{k}$  of the BZ, except for the center  $\Gamma$  where such a behavior is reversed. The qualitative change observed in the ED results is remarkably reproduced by the SCBA. This concordance gives a strong support to our analytical approach and so, from now on, we will focus on the SCBA spectra in the thermodynamic limit.

The spectral function structures shown in Fig. 2 can be traced back to the distinct hole motion processes mentioned above. The spectra extend over a frequency range of  $\sim 9t$ , that is, the non-interacting electronic bandwidth. Similar values have been found in the experiments on the silicon surfaces[1, 2]. For momentum  $\Gamma$  (upper panel) both processes contribute coherently to the quasiparticle excitation at the top of the spectra. In an energy range of  $\sim 2J$  just above the QP energy, there are other noticeable resonances of magnetic origin, reminiscent of the string-like ones found in non-frustrated antiferromagnets[8, 14]. There is also a small incoherent component centered around  $6t$  below the QP peak. When moving away from  $\Gamma$ , there is a spectral weight transfer from the low energy coherent sector to higher energies. At  $M'$  (middle panel) the coherence is completely lost, surviving only a magnetic tail at low energy and a structureless background. At  $K$  (lower panel), corresponding to the magnetic vector  $\mathbf{Q}$ , the coherence emerges once again, giving rise to the QP and the low energy resonances. In the background there is a broad resonance related to the free hopping hole motion with a finite lifetime of order  $\sim 4J$ .

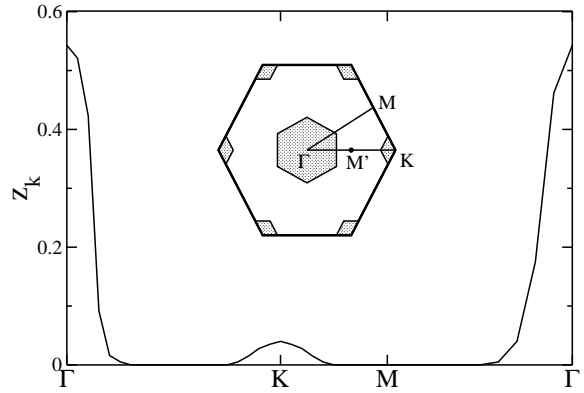


FIG. 3: QP intensity along the  $\Gamma - K - M - \Gamma$  path for  $J/t = 0.4$ . Inset:  $\sqrt{3} \times \sqrt{3}$  Brillouin zone. In the shaded areas the QP weight is finite.

In Fig. 3 we show the intensity of the QP peak along high symmetry axes and, in the inset, the region of the BZ where the quasiparticle weight is finite for  $J/t = 0.4$ . Besides the strong  $\mathbf{k}$ -dependence, it can be observed that there is no QP for momenta outside the neighborhood of the magnetic Goldstone modes ( $\mathbf{k} = \mathbf{0}, \mathbf{Q}$ ). The presence of QP in the non-equivalent vertices of the BZ is an artifact of the used approximation: the magnetic ground state has a definite chirality ( $\mathbf{Q}$ ), but our vertex interaction does not discriminate between  $\pm \mathbf{Q}$  resulting the whole spectral function degenerate in both momenta. Actually, the experiments should detect a well-defined chirality, leading to a QP signal only at  $\mathbf{Q}$  and equivalent points generated under reciprocal vector translations of the  $\sqrt{3} \times \sqrt{3}$  triangular lattice. The non existence of quasiparticle is a striking manifestation of the strong interference between the free and magnon-assisted hopping processes. The coherence of the QP is lost because of the quite different group velocities of the spin fluctuations and the tight-binding hole motion[15].

The available photoemission spectroscopy data for the silicon surfaces have a low energy resolution ( $\sim 100-200$  meV) [1, 2] and it is impossible to discern the energy structure of the surface spectra. The surface bands obtained experimentally are correctly reproduced by the center-of-mass of our spectra. The latter coincides with the free hopping dispersion (see Fig. 4) as it is expected from the exact treatment of the first spectral moment of our theory. Using the transfer integral  $t$  obtained from first-principles calculations, our bandwidths compare very well with the experimental ones, reflecting the narrowing induced by the electronic correlation. For the  $K/\text{Si-B}$  (SiC) surface we have obtained  $W \sim 0.3$  eV ( $\sim 0.18$  eV). Nowadays, state-of-the-art ARPES experiments would provide a higher energy resolution of the surface state bands[16]. In particular, the spectra structures caused by the assumed magnetic order predicted above (Fig. 3) could be detected at temperatures well

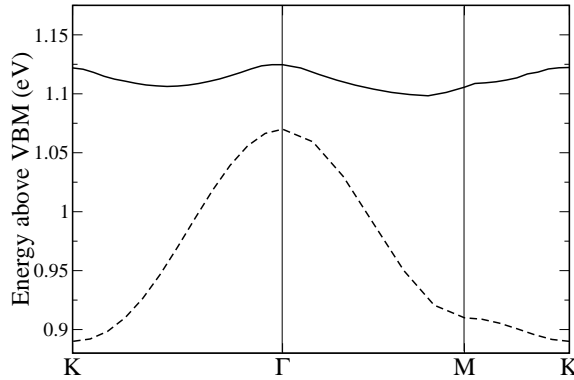


FIG. 4: Surface band structure for the SiC(0001)-( $\sqrt{3} \times \sqrt{3}$ ) surface. The solid line is the photothreshold energy (QP dispersion, when it exists) and the dashed one is the center-of-mass spectra band. Energies are given relative to the measured bulk valence-band maximum (VBM). Experimentally the Fermi level is located at 2.3 eV above the VBM

below  $J \sim 150$  K ( $\sim 40$  K). Another observable magnetic implication is the position of the spectral function local minima in momentum space. In Fig. 4 we show the center-of-mass and the photothreshold dispersions for the SiC surface. When the quasiparticle exists, the photothreshold corresponds to the QP energy excitation. As it can be observed, the underlying magnetic structure changes the center-of-mass minimum at the  $K$  point to a QP energy local maximum, nearly degenerate with the hole ground state momentum  $\Gamma$ . There is also an appreciable reduced bandwidth  $\sim 10$  meV of the photothreshold dispersion in comparison with the measured surface state bandwidth  $\sim 200$  meV. Whereas for the K/Si-B surface the values are  $\sim 40$  meV and  $\sim 300$  meV, respectively.

In conclusion, we have studied theoretically the photoemission spectra of the triangular silicon surfaces SiC(0001)-( $\sqrt{3} \times \sqrt{3}$ ) and K/Si(111)- $\sqrt{3} \times \sqrt{3}$  assuming the presence of a long-range magnetic Néel order. Recently, the very existence of magnetic order has been under debate. Our theoretical predictions can provide useful ground to the analysis of future improved photoemission experiments. Using a simple and reliable analytical method (SCBA), we have obtained clear signatures of interesting physics caused by strong electronic correlation on simple silicon surfaces.

In addition, it would be interesting to investigate the effect of further doping on these surfaces, as a labora-

tory for non-Fermi liquid theories. Experimentally, the finite doping could be easily accomplished by monitoring the coverage of potassium on the Si-B(111) surface. Finally, there is another kind of quasi 2D triangular insulating compounds that have recently been shown to behave non-conventionally, like  $Cs_2CuCl_4$  [17] with fractional spin excitations and the organic superconductor family ( $BEDT-TTF$ )<sub>2</sub> $X$  [18]. We think our findings could stimulate further theoretical and experimental work on these materials in the hole doped regime.

We acknowledge H. H. Weitering for useful communication. This work was done under PICT Grant No. N03-03833 (ANPCyT) and was partially supported by Fundación Antorchas.

---

- [1] H. H. Weitering *et al.*, Phys. Rev. Lett. **78**, 1331 (1997).
- [2] L. I. Johansson, F. Owman, and P. Mårtensson, Surf. Sci. **360**, L478 (1996).
- [3] G. Santoro, S. Scandolo, and E. Tosatti, Phys. Rev. B **59**, 1891 (1999); V. I. Anisimov *et al.*, Phys. Rev. B **61**, 1752 (2000).
- [4] J. Northrup and J. Neugebauer, Phys. Rev. B **57**, R4230 (1998).
- [5] C. S. Hellberg and S. C. Erwin, Phys. Rev. Lett. **83**, 1003 (1999).
- [6] P. W. Anderson, Science **235**, 1196 (1987); R. B. Laughlin, Phys. Rev. Lett. **79**, 1726 (1997).
- [7] B. O. Wells *et al.*, Phys. Rev. Lett. **74**, 964 (1995).
- [8] G. Martinez and P. Horsch, Phys. Rev. B **44**, 317 (1991); Z. Liu and E. Manousakis, Phys. Rev. B **45**, 2425 (1992).
- [9] C. L. Kane, P. A. Lee, and N. Read, Phys. Rev. B **39**, 6880 (1989).
- [10] M. Azzouz and Th. Dombre, Phys. Rev. B **53**, 402 (1996); W. Apel, H. U. Everts, and U. Körner, Eur. Phys. J. B **5**, 317 (1998); M. Vojta, Phys. Rev. B **59**, 6027 (1999).
- [11] We have used lattice sizes up to 2700 sites.
- [12] V. Ramachandran and R. M. Feenstra, Phys. Rev. Lett. **82**, 1000 (1999).
- [13] M. Capone, L. Capriotti, F. Becca, and S. Caprara, Phys. Rev. B **63**, 85104 (2001).
- [14] M. Brunner, F. Assaad, and A. Muramatsu, Phys. Rev. B **62**, 15480 (2000).
- [15] L. O. Manuel *et al.*, in preparation.
- [16] H. H. Weitering, private communication.
- [17] R. Coldea, D. A. Tennant, A. M. Tsvelik, and Z. Tylicki, Phys. Rev. Lett. **86**, 1335 (2001).
- [18] R. H. McKenzie, Science **278**, 820 (1997); Comments Cond. Mat. **18**, 309 (1998).